SCIENCE CHINA
Information Sciences

• RESEARCH PAPER •

August 2017, Vol. 60 082402:1–082402:6
doi: 10.1007/s11432-016-0539-6

Ultra-compact tunable graphene-based plasmonic multimode interference power splitter in mid infrared frequencies

Pingping QIU[1], Weibin QIU[1*], Zhili LIN[1], Houbo CHEN[1], Yixin TANG[1], Jiaxian WANG[1], Qiang KAN[2] & Jiaoqing PAN[2]

[1]*College of Information Science and Engineering, Huaqiao University, Xiamen* 361021*, China;*
[2]*Institute of Semiconductors, Chinese Academy of Sciences, Beijing* 100083*, China*

Received October 15, 2016; accepted December 2, 2016; published online February 20, 2017

Abstract In this paper, we propose graphene-based plasmonic multimode interference power splitters with ultra-compact size working in mid infrared range. Further, the arbitrary-ratio 1×2 power splitter with a size of 140 nm×232 nm, where the splitting ratio can be tuned continuously from 1:1 to 100:0, is numerically demonstrated. Meanwhile, the graphene-based arbitrary-ratio 1×2 power splitters with different frequencies and chemical potentials are also investigated. The proposed multimode interference structure with a deep nanoscale footprint might be a fundamental component of the future high density integrated plasmonic circuit or on-chip plasmonic interconnect techniques.

Keywords graphene, multimode interference, surface plasmon polaritons, power splitter, plasmonic integrated circuits

Citation Qiu P P, Qiu W B, Lin Z L, et al. Ultra-compact graphene-based plasmonic multimode interference power splitter in mid infrared frequencies. Sci China Inf Sci, 2017, 60(8): 082402, doi: 10.1007/s11432-016-0539-6

1 Introduction

In the past decades, multimode interference (MMI) couplers have been widely applied to integrated photonics systems due to the compact footprint [1], wide optical bandwidth, insensitivity to the input polarization [2] and low excess loss [3]. The MMI coupler offers broad fields applications, such as polarization splitters/combiners [4], (de)multiplexer [5–7], all-optical switch [8], optical power splitters/combiners [9], and so on [10–13]. Unlike the conventional MMI power splitter which can only obtain a few discrete splitting ratios [14, 15], an arbitrary-ratio 1×2 power splitter can be realized by breaking the symmetry of interference [12], which leads to a great number of applications in optoelectronic integrated circuits, including on-chip power monitoring [16], an asymmetric Mach-Zehnder interferometer (MZI) modulator [17], and optical filters [18].

Recently, graphene, a monolayer of carbon atoms which are densely packed in a two-dimensional (2D) honeycomb lattice [19, 20], has been shown to possess unique electronic and optical properties which can

* Corresponding author (email: wbqiu@hqu.edu.cn)

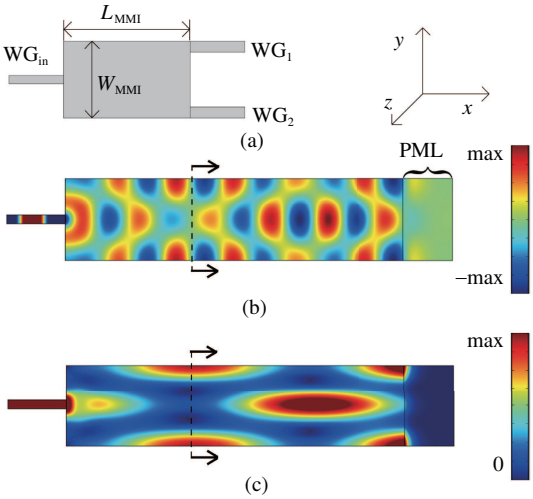

Figure 1 (Color online) (a) The schematic of 1×2 power splitter; (b) the magnetic field (H_z) distribution of 1×2 power splitter; (c) the normalized optical energy flux density distribution of 1×2 power splitter, with an operation mid infrared frequency of 6e13 Hz (5 μm) and a chemical potential of 0.6 eV respectively. The width and length of WG_{in} are 15 nm and 100 nm respectively, width and length of output waveguides of 1×2 power splitter are 20 nm and 100 nm respectively. The perfect matched layers (PML) prevent the plasmonic field reflected back from the right end of the MMI waveguides.

be modified by changing chemical potential of graphene [21, 22], via chemical doping or electrical gating [23]. Graphene plasmonic waveguides based MMI splitters [24] have been studied which show a broadband tenability. Besides, the strong confinement ability of graphene can constrain the electromagnetic field in nanoscale, which leads to an ultra-compact size of the device and high integrated density.

The operation principle of MMI couplers is based on the so-called self-imaging effect [25]. An input field profile is reproduced in single or multiple images at periodic intervals in a multimode waveguides along the field propagation direction of the waveguide. By using self-imaging effect, one incident light can be coupled into multiple output waveguides, resulting in an optical power splitter or combiner.

In this paper, we present the design and numerical analysis of graphene-based 1×2 plasmonic MMI power splitter. Simulation results, obtained by COMSOL Multiphysics RF Module, version 4.3b, commercial software, reveal that stable two-fold images can be obtained clearly with ultra-compact size and wide operation bandwidth. Furthermore, we studied a graphene-based arbitrary-ratio 1×2 power splitter which is realized by breaking the symmetry of interference, i.e., cutting one of the left corners in the multimode region. Meanwhile, graphene-based arbitrary-ratio 1×2 power splitters with various frequencies and chemical potentials are also numerically studied.

2 Simulation methods and models

Figure 1(a) shows the schematic of 1×2 power splitter formed by a single-layer graphene. Transverse magnetic (TM) mode is, through input waveguide (WG_{in}, located at the center of the left edge of multimode region), transmitted into multimode region where the constructive interference of multiple modes is excited. Then, the TM mode is coupled into output waveguides (WG_1 and WG_2, located at the upper and underside of right edge of multimode region where the first two-fold images formed.), resulting in a power splitter. Furthermore, the constructive interference excited in multimode region including general interference and restricted interference, can be specifically classified as restricted interference, where certain modes are excited alone in our case [25]. This realized a reduced length periodicity of mode phase factor, which leads to a compact size of the device. The width and length of WG_{in} are 15 nm and 100 nm respectively, width and length of output waveguides of 1×2 power splitter are 20 nm and 100 nm respectively.

As for MMI device, the wider the width of multimode region becomes, the more modes can be excited in the multimode region, which means a better self-imaging quality is expectable. Meanwhile, the footprint

of device becomes larger. Consequently, to obtain a trade-off between the self-imaging quality and the size of device, we choose W_{MMI} =140 nm for 1×2 power splitter, the corresponding L_{MMI} = 232 nm. Figure 1(b) shows the resulting magnetic field (H_z) distribution of 1×2 power splitter at $\mu_{\mathrm{c}} = 0.6$ eV with an operation mid infrared frequency of 6×10^{13} Hz, Figure 1(c) is the corresponding normalized optical energy flux density distribution, which reveals that stable two-fold images can be clearly obtained by our proposed models. In order to obtain a more accurate field distribution, the perfectly matched layer (PML) which acts as a non-reflecting boundary condition, is set here. According to Soldano et al. [25], the N-fold image distance L_{MMI} is expressed as

$$L_{\mathrm{MMI}} = \frac{3ML_{\pi}}{4N}, \tag{1}$$

where M and N are any positive integers with no common divisor. L_{π} is the beat length between the two lowest-order modes, which can be written as

$$L_{\pi} \approx \frac{4n_{\mathrm{eff}}W_{\mathrm{MMI}}^2}{3\lambda}, \tag{2}$$

where W_{MMI} is the width of the multimode region, λ (= c/f) is the working wavelength, and n_{eff} is the effective index of the multimode region, i.e., the effective index of graphene which is given by

$$n_{\mathrm{eff}} = \frac{\beta}{k_0}, \tag{3}$$

where k_0 is the wave number in free space. As for TM mode, the propagation constants of surface plasmon polaritons, supported by a single-layer graphene, can be expressed as [26, 27]

$$\beta = k_0\sqrt{1 - \left(\frac{2}{\eta_0\sigma_{\mathrm{g}}}\right)^2}, \tag{4}$$

where η_0 (377 Ω) is impedance of air, which can be expressed as $(\mu_0/\varepsilon_0)^{1/2}$ where μ_0 and ε_0 are permeability and permittivity of vacuum respectively. The surface conductivity of graphene σ_{g} which consists of the interband electron transitions σ_{inter} and the intraband electron-photon scattering σ_{intra}, can be obtained from the Kubo formula [27–29],

$$\sigma_{\mathrm{g}} = \sigma_{\mathrm{intra}} + \sigma_{\mathrm{inter}}, \tag{5}$$

with

$$\sigma_{\mathrm{intra}} = \frac{-\mathrm{i}e^2k_{\mathrm{B}}T}{\pi\hbar^2(\omega - i/\tau)}\left[\frac{\mu_{\mathrm{c}}}{k_{\mathrm{B}}T} + 2\ln\left(1 + \exp\left(-\frac{\mu_{\mathrm{c}}}{k_{\mathrm{B}}T}\right)\right)\right], \tag{6}$$

$$\sigma_{\mathrm{inter}} = \frac{-\mathrm{i}e^2}{2h}\ln\left[\frac{2\left|\mu_{\mathrm{c}}\right| - \hbar(\omega - i/\tau)}{2\left|\mu_{\mathrm{c}}\right| + \hbar(\omega - i/\tau)}\right], \tag{7}$$

where μ_{c} is the chemical potential, ω is the angular frequency of the plasmon, e is the electron charge, k_{B} is the Boltzmann constant, $T = 300$ K is the temperature, $\hbar = h/2\pi$ is the reduced Planck's constant, and τ is the electron momentum relaxation time. Specifically, the chemical potential of graphene can be tuned via chemical doping or electrical gating [23]. Efetov et al. [30] experimentally demonstrated that a chemical potential as high as 2 eV can be achieved. Also, it has been shown that high-quality suspended graphene with direct current mobility as high as 10^5 $\mathrm{cm^2V^{-1}s^{-1}}$ can be obtained, which leads to $\tau >$ 1.5 ps [31]. In this paper, we set $\mu_{\mathrm{c}} = 0.6$ eV, 0.7 eV, and $\tau = 0.5$ ps, which is conservative enough to ensure the reliability of our numerical study.

In order to realize the tunability of the power splitting ratio, as can be seen from Figure 2(a), we remove a rectangle with width of W_{r} and length of L_{r} from the left bottom of the multimode region on the basis of the structure shown in Figure 1(a). Varied power splitting ratios can be obtained by modifying the area of the removed rectangle. As shown in Figure 2(b) and (c), one can see that the intensity of the magnetic field and the normalized optical energy flux density from two output waveguides are not equal any more when a rectangle removed, which implies an achievement of the effective tunability of the splitting ratio in our proposed structure.

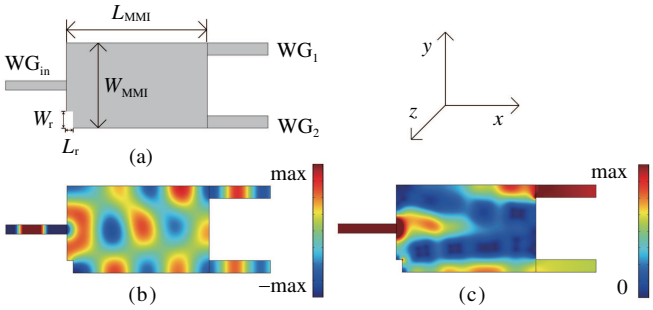

Figure 2 (Color online) (a) Schematic of 1×2 power splitter with a rectangle removed; (b) and (c) are the corresponding H_z distribution and the normalized optical energy flux density distribution with an operation mid infrared frequency of 6e13 Hz (5 μm) and a chemical potential of 0.6 eV, $L_r = 10$ nm, $W_r = 20$ nm. The other geometrical parameters are the same as structure shown in Figure 1(a).

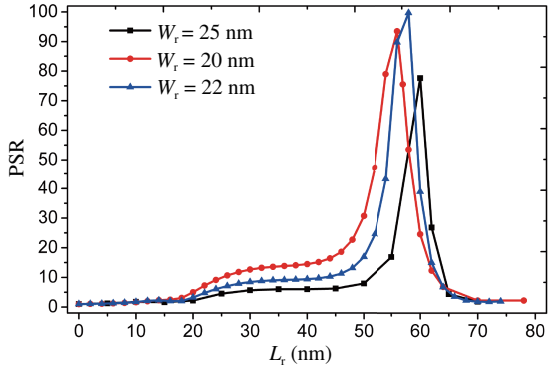

Figure 3 (Color online) The PSRs of 1×2 power splitter at 6e13 Hz, $\mu_c = 0.6$ eV with the W_r being 20, 22 and 25 nm respectively.

3 Discussion and analysis

An arbitrary-ratio 1×2 power splitter can be accomplished through breaking the symmetry of the multimode region [12]. The splitting ratio of the power splitter (PSR, defined as the power of the WG_1 divides the power of WG_2) is tuned by cutting varying area in the left bottom of the multimode region. In a certain range, the larger area we removed, the bigger splitting ratio we can obtain. To obtain an arbitrary-ratio power splitter, the W_r should be chosen properly. As shown in Figure 3, a 99.7:1 PSR can be obtained at 6×10^{13} Hz, $\mu_c = 0.6$ eV via changing the L_r with the W_r being 22 nm. At $L_r = 34$ nm and $W_r = 22$ nm, a 90:10 PSR can be obtained. It is obviously that a 50:50 PSR can be obtained when there is no rectangle removed. As for the other two curves with the W_r of 20 nm and 25 nm, only 99.5:1 and 77.5:1 PSRs can be achieved via tuning the L_r respectively. We also can see the H_z distribution and the normalized optical energy flux density distribution of 1×2 power splitters with a 20 nm×10 nm area removed from multimode region shown in Figure 2, which demonstrate that a quite well splitting ability can be realized for the power splitters we proposed, especially for those circumstances that continuous arbitrary splitting ratios are required.

On the other hand, arbitrary-ratio power splitters can be realized with different operation frequencies in the same way. 5.6×10^{13}, 5.8×10^{13} and 6.0×10^{13} Hz (5.36, 5.17 and 5.00 μm) are chosen as the operation frequencies with the W_r of 30, 18 and 22 nm respectively, the simulation results reveal that the PSRs can be successfully tuned from 1:1 to 109.1:1, 1:1 to 109.4:1 and 1:1 to 99.7:1 respectively via modifying L_r, which agree quite well with the results we obtained above. Figure 4(a) shows the resulting simulations of the arbitrary-ratio 1×2 power splitter at different frequencies with chemical potential of 0.6 eV.

Further, the chemical potential, as one of the key parameters of graphene, is considered. Figure 4(b) plots the PSRs of 1×2 power splitters at 6×10^{13} Hz with chemical potencials being 0.6 and 0.7 eV, the

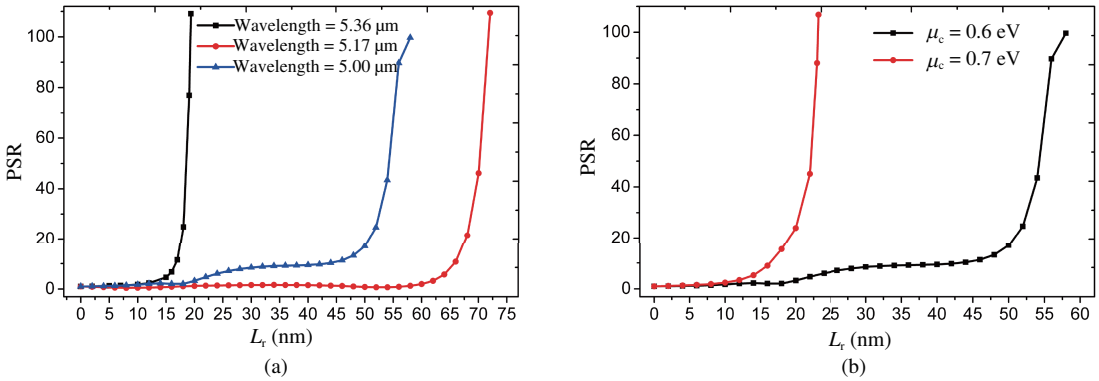

Figure 4 (Color online) (a) The PSRs of 1×2 power splitter at $\mu_c = 0.6$ eV with operation frequencies of 5.6e13, 5.8e13 and 6e13 Hz (5.36, 5.17 and 5.00 μm) respectively; (b) the PSRs of 1×2 power splitter at 6e13 Hz with chemical potentials of 0.6 and 0.7 eV respectively.

corresponding PSRs can be tuned form 1:1 to 99.7:1 and 1:1 to 106.8:1 respectively, which demonstrates that continuous PSRs from 1:1 to 100:0 can be realized, which offers another design parameter for our proposed arbitrary-ratio power splitter.

According to self-imaging effect [25], such asymmetric MMI, excited by asymmetric perturbation in the multimode region, has a significantly different and asymmetric optical phase and field distribution, which is rooted from the partial coherence of asymmetric coherence between the fundamental mode and the higher order eigen modes of the multimode waveguide region. And this finally leads to an arbitrary splitting ratio via tuning the area of the removed rectangle. The effect of the removed part of multimode waveguide region is always relied on its area and refractive index. Graphene's refractive index is determined by the frequency and chemical potential. So changing in the area, working frequency and chemical potential of graphene leads to the changing of beating length, then changes the beating length related mode phase factor, eventually affected the constructive interference excited in multimode region, resulting in different splitting ratios. Practically, the fabrication way of the proposed structure can follow the method proposed in [32], where the graphene monolayer seats on a SiO_2 on Si substrate. Expected chemical potential can be obtained by applying external electric field. So the proposed MMI structure is achieved.

4 Conclusion

In conclusion, graphene-based 1×2 MMI power splitter with ultra-compact size of 140 nm×232 nm, was studied in this paper. Stable two-fold images can be clearly obtained at 6e13 Hz with a chemical potential of 0.6 eV by our proposed models. Further, we emphatically discussed about the graphene-based arbitrary-ratio 1×2 MMI power splitter, whose splitting ratio can be tuned from 1:1 to 100:0 continuously. Moreover, the 1×2 power splitters are numerically simulated and analyzed at different operation frequencies and chemical potentials. The resulting simulations demonstrate that an arbitrary PSR can be obtained by our proposed MMI power splitter. The proposed structure might be a fundamental component in the future high density plasmonic integrated circuit or on-chip plasmonic interconnect techniques.

Acknowledgements The authors are grateful to the support by Natural Science Fund of China (Grant No. 61378058), Science and Technology Fund of Quanzhou (Grant No. Z1424009), Fujian Province Science Fund for Distinguished Young Scholars (Grant No. 2015J06015), Promotion Program for Young and Middle-Aged Teachers in Science and Technology Research of Huaqiao University (Grant No. ZQN-YX203) and Project for Cultivating Postgraduates' Innovative Ability in Scientific Research of Huaqiao University (Grant No. 1511301022).

Conflict of interest The authors declare that they have no conflict of interest.

References

1 Halir R, Roelkens G, Ortega-Monux A, et al. High-performance 90 degrees hybrid based on a silicon-on-insulator multimode interference coupler. Opt Lett, 2011, 36: 178–180
2 Truong C D, Tran D H, Le T T. Design of an insensitive-polarization all-optical switch based on multimode interference structures. Photonic Nanostruct-Fund Appl, 2013, 11: 210–216
3 Sheng Z, Wang Z, Qiu C, et al. A compact and low-loss MMI coupler fabricated with CMOS technology. IEEE Photonic J, 2012, 4: 2272–2277
4 Swillam M A, Bakr M H, Li X. Efficient design of integrated wideband polarization splitter/combiner. J Lightw Tech, 2010, 28: 1176–1183
5 Zhu Z, Garcia-Ortiz C E, Han Z, et al. Compact and broadband directional coupling and demultiplexing in dielectric-loaded surface plasmon polariton waveguides based on the multimode interference effect. Appl Phys Lett, 2013, 103: 61108
6 Prajzler V, Nekvindova P, Varga M, et al. Design of 1X2 wavelength demultiplexer based on multimode interference. J Optoelectron Adv M, 2014, 16: 1226–1231
7 Li Y M, Li C, Li C B, et al. Compact two-mode (de)multiplexer based on symmetric Y-junction and multimode interference waveguides. Opt Express, 2014, 22: 5781
8 Tajaldini M, Jafri M Z M. An optimum multimode interference coupler as an all-optical switch based on nonlinear modal propagation analysis. Optik-Int J Light Electron Optics, 2015, 126: 436–441
9 Tajaldini M, Jafri M Z M. Simulation of an ultra-compact multimode interference power splitter based on Kerr nonlinear effect. J Lightw Tech, 2014, 32: 1282–1289
10 Rodriguez-Rodriguez A, Dominguez-Cruz R, May-Arrioja D A, et al. Fiber optic refractometer based in multimode interference effects (MMI) using Indium Tin Oxide (ITO) coating. In: Proceedings of IEEE Sensors, Busan, 2015. 1–3
11 Morrissey P E, Peters F H. Multimode interference couplers as compact and robust static optical phase shifters. Opt Commun, 2015, 345: 1–5
12 Deng Q Z, Liu L, Li X B, et al. Arbitrary-ratio 1 X 2 power splitter based on asymmetric multimode interference. Opt Lett, 2014, 39: 5590–5593
13 Gordón C, Guzman R, Leijtens X, et al. On-chip mode-locked laser diode structure using multimode interference reflectors. Photonic Res, 2015, 3: 15–18
14 Zhou J T, Shen H J, Jia R, et al. Uneven splitting-ratio 1 X 2 multimode interference splitters based on silicon wire waveguides. Chinese Opt Lett, 2011, 9: 82303
15 Bachmann M, Besse P A, Melchior H. Overlapping-image multimode interference couplers with a reduced number of self-images for uniform and nonuniform power splitting. Appl Opt, 1995, 34: 6898–6910
16 Zanzi A, Brimont A, Griol A, et al. Compact and low-loss asymmetrical multimode interference splitter for power monitoring applications. Opt Lett, 2016, 41: 227–229
17 Yi H X, Long Q F, Tan W, et al. Demonstration of low power penalty of silicon Mach-Zehnder modulator in long-haul transmission. Opt Express, 2012, 20: 27562–27568
18 Matsuo S, Yoshikuni T, Segawa T, et al. A widely tunable optical filter using ladder-type structure. IEEE Photonic Tech Lett, 2003, 15: 1114–1116
19 Grigorenko A N, Polini M, Novoselov K S. Graphene plasmonics. Nature Photonic, 2012, 6: 749–758
20 Novoselov K S, Geim A K, Morozov S V, et al. Electric field effect in atomically thin carbon films. Science, 2004, 306: 666–669
21 Luo X, Zhai X, Wang L L, et al. Narrow-band plasmonic filter based on graphene waveguide with asymmetrical structure. Plasmonics, 2015, 10: 1427–1431
22 Shang X J, Zhai X, Li X F, et al. Realization of graphene-based tunable plasmon-induced transparency by the dipole-dipole coupling. Plasmonics, 2016, 11: 419–423
23 Vakil A, Engheta N. Transformation optics using graphene. Science, 2011, 332: 1291–1294
24 Zheng R Q, Gao D S, Dong J J. Ultra-compact and broadband tunable mid-infrared multimode interference splitter based on graphene plasmonic waveguide. In: Proceedings of Asia Communications and Photonics Conference, Hong Kong, 2015
25 Soldano L B, Pennings E. Optical multi-mode interference devices based on self-imaging: principles and applications. Lightw Tech, 1995, 13: 615–627
26 Wang B, Zhang X, Yuan X C, et al. Optical coupling of surface plasmons between graphene sheets. Appl Phys Lett, 2012, 100: 131111
27 Huang Y X, Qiu W B, Lin S X, et al. Investigation of plasmonic whispering gallery modes of graphene equilateral triangle nanocavities. Sci China Inf Sci, 2016, 59: 042413
28 Hanson G W. Dyadic Green's functions and guided surface waves for a surface conductivity model of graphene. J Appl Phys, 2008, 103: 64302
29 Qiu W B, Liu X H, Zhao J, et al. Nanofocusing of mid-infrared electromagnetic waves on graphene monolayer. Appl Phys Lett, 2014, 104: 041109
30 Efetov D K, Kim P. Controlling electron-phonon interactions in graphene at ultrahigh carrier densities. Phys Rev Lett, 2010, 105: 256805
31 Zhang T, Chen L, Wang B, et al. Tunable broadband plasmonic field enhancement on a graphene surface using a normal-incidence plane wave at mid-infrared frequencies. Sci Rep-UK, 2015, 5: 11195
32 Shi B, Cai W, Zhang X Z, et al. Tunable band-stop filters for graphene plasmons based on periodically modulated graphene. Sci Rep-UK, 2016, 6: 26796